BHE Field Design by Superposition of Effects in Space and Time

S. Lazzari[*1], E. Zanchini[1]
[1]DIENCA, Università di Bologna
*Corresponding author: DIENCA, Viale Risorgimento 2, I-40136, Bologna, Italy; stefano.lazzari@unibo.it

Abstract: The long-term time evolution of the mean surface temperature of the most critical BHE, for BHE fields with arbitrarily given monthly heat loads and no groundwater flow, is studied by means of finite-element computations performed through COMSOL Multiphysics and the superposition of effects. A unit step heat load, with duration of one month, is considered, and its effects are evaluated. Then, the effects of any periodic heat load with a period of one year and given monthly heat loads can be obtained by a weighted sum of the effects of the unit step heat load, properly displaced in time. The result of the computations is a set of dimensionless equations that, properly superimposed, yield the time evolution of the dimensionless temperature at the interface between the most critical BHE and the ground, for a period of 50 years, for several typical configurations of BHE fields.

Keywords: Borehole Heat Exchanger (BHE) Fields, Design Method, Superposition Principle, Finite Element Simulations.

1. Introduction

In order to reduce the use of fossil fuels and its environmental effects, ground coupled heat pumps are becoming an important technology for building heating and cooling, and are widely studied in the literature. The heat exchangers with the ground can be either horizontal or vertical. The vertical heat exchangers, called Borehole Heat Exchangers (BHEs), are usually composed of a drilled hole where either a single polyethylene U-tube or two U-tubes are inserted; water or a mixture of water and glycol flows in the tubes. The hole is then sealed by a proper grout. BHEs can also be composed of two coaxial tubes, namely an outer tube, usually made of steel, and an inner polyethylene tube.

The design of a BHE field is usually performed by employing the method developed by Kavanaugh and Rafferty [1] and recommended by ASHRAE [2]. This method refers to a period of 10 years and does not consider any groundwater movement. Therefore, it cannot ensure the long-term sustainability of BHE fields with unbalanced seasonal loads, or take into account the effects of the groundwater movement on the long-term sustainability.

For a single BHE with completely unbalanced seasonal loads, the long-term sustainability has been verified both experimentally and theoretically, even in the absence of groundwater movement [3, 4]. Other studies [5, 6] have shown that medium or large BHE fields with unbalanced seasonal loads, in the absence of groundwater movement, can reach a critical condition in a few decades.

Chiasson, Rees and Spitler [7] presented a first analysis of the effects of groundwater flow on a single BHE and on a BHE field, showing that a speed of 60 m / year, typical for a coarse sand, may have considerable effects in the long term sustainability, while higher speeds are required to influence the effective thermal conductivity of the soil. Zanchini, Lazzari and Priarone [8] recently studied the effects of groundwater movement on large BHE fields, by considering the limiting case of infinite BHEs placed in a single line, in a double line or in a quadruple line, and showed that even a very slow groundwater flow can ensure the long term sustainability of large BHE fields.

Although large BHE fields with completely (or nearly completely) unbalanced seasonal heat loads must be avoided, because they should be shut down after some decades [6, 8], small or medium BHE fields with partially balanced seasonal loads appear as feasible, even in the absence of groundwater movement. For these fields, the ASHRAE design method does not ensure the long term sustainability and alternative design methods are required.

In this paper, a method to evaluate the long term performance of BHE fields with unbalanced seasonal heat loads and no groundwater movement is presented. This method allows to determine, for a period of 50 years, the mean temperature of the interface between the most critical BHE and the ground, with reference to any BHE field, subjected to a time periodic heat load with a period of one year and arbitrarily

given monthly heat loads. The method is based on the time superposition of twelve constant heat loads with duration of one month each. The design of a BHE field requires also the analysis of the effects of the hourly peak loads, which can be performed by a method already available (although with a different definition of the Fourier number) in Ref. [8]. The results are given in dimensionless form, as tables of coefficients of two equations, and can be quickly implemented in Excel.

2. Governing equations and numerical modeling

Let us consider a BHE field subjected to a heat load slowly variable in time, so that the heat capacity of each BHE is not relevant. Accordingly, the time evolution of the mean temperature of the surface between a BHE and the ground can be evaluated by replacing the real BHE by a cylindrical heat source, with the same diameter as the BHE. Then, let us consider the ground as an infinite solid medium with constant thermo-physical properties, where no groundwater movement takes place. Moreover, if one neglects the axial temperature gradient, the heat transfer problem becomes 2D and each BHE in the field can be sketched as a circular heat source in an infinite solid medium. Finally, let us study only one BHE: the temperature changes in the ground due to the surrounding BHEs will be evaluated by applying the superposition of effects in space.

Let us adopt a Cartesian reference frame centered in the axis of the BHE and a square computational domain around the BHE, with a side equal to 2000 times the BHE diameter D.

At the initial instant of time, $\tau = 0$, the temperature T is uniform and equal to the undisturbed ground temperature, T_g. For $\tau > 0$, a uniform heat flux per unit area is applied to the boundary surface between BHE and ground, given by

$$q(\tau) = \frac{Q_0}{\pi D} F(\tau) \quad , \tag{1}$$

where Q_0 is the highest (lowest if negative) heat flux per unit length applied to the BHE and $F(\tau)$ is a dimensionless function of time; Q_0 is positive if heat is supplied to the ground (summer operation).

The differential equation to be solved is

$$\frac{\partial T}{\partial \tau} = \alpha_g \nabla^2 T \quad , \tag{2}$$

where α_g is the thermal diffusivity of the ground. The boundary condition at the surface S_B between BHE and ground is

$$-k_g \left(\nabla T \cdot \mathbf{n}\right)\Big|_{S_B} = \frac{Q_0}{\pi D} F(\tau) \quad , \tag{3}$$

where $\mathbf{n}$ is the outward unit normal; the external boundary of the computational domain is considered as adiabatic. By introducing the dimensionless operator $\nabla^* = D\,\nabla$ and the dimensionless quantities

$$x^* = \frac{x}{D},\ y^* = \frac{y}{D},\ \tau^* = \frac{\alpha_g \tau}{D^2},\ T^* = k_g \frac{T - T_g}{Q_0}, \tag{4}$$

one can rewrite Eqs. (2) and (3) in the following dimensionless form:

$$\frac{\partial T^*}{\partial \tau^*} = \nabla^{*2} T^* \quad , \tag{5}$$

$$-\left(\nabla^* T^* \cdot \mathbf{n}\right)\Big|_{S_B} = \frac{1}{\pi} F(\tau) \quad . \tag{6}$$

Obviously, the dimensionless initial condition is $T^* = 0$ in the whole computational domain.

A BHE field is used together with a heat pump for the yearly air-conditioning of a building. Thus, with a good approximation, the BHEs are subjected to a time periodic heat load, with a period $\tau_0 = 1$ year, that accounts for the thermal energy that has to be exchanged with the ground during the year to help maintaining the desired air conditions inside the building. Typically, the evaluation of this thermal energy is made on a monthly basis.

According to this interpretation and with reference to Fig.1, let us assume that $F(\tau)$ is a unit step function with a duration of one month, which is given by the following sum of two Heaviside step functions:

$$F(\tau) = H(\tau) - H(\tau - \tau_1) \quad , \qquad (7)$$

where τ_1 = 1 month. By a time superposition of twelve functions like $F(\tau)$, each of them shifted forth by τ_1 and properly weighted, one obtains a dimensionless heat load having a duration of τ_0 = 1 year, and arbitrarily given monthly loads. Indeed, by employing the notation

$$\begin{aligned} F(\tau - \tau_1) &= H(\tau - \tau_1) - H(\tau - 2\tau_1) \\ F(\tau - 2\tau_1) &= H(\tau - 2\tau_1) - H(\tau - 3\tau_1) \quad , (8) \\ &\ldots\ldots \end{aligned}$$

one can write the dimensionless heat load during one year as

$$\begin{aligned} &A_0 F(\tau) + A_1 F(\tau - \tau_1) + A_2 F(\tau - 2\tau_1) + \\ &\ldots\ldots + A_{11} F(\tau - 11\tau_1) = \sum_{j=0}^{11} A_j F(\tau - j\tau_1) \end{aligned} \qquad (9)$$

where A_0, A_1,…, A_{11} are dimensionless weighting coefficients that account for the thermal energy that has to be exchanged with the ground during the considered month (see Fig.2 for an example). Finally, this yearly heat load can be superposed in time in order to obtain a time-periodic heat load $f(\tau)$, with a period τ_0 of one year (Fig.3)

$$f(\tau) = \sum_{i=0}^{N} \sum_{j=0}^{11} A_j F(\tau - i\tau_0 - j\tau_1) \qquad (10)$$

where N is the number of years considered.

To state the problem in a dimensionless form which holds for different ground and BHE diameter, it is useful to introduce the Fourier number

$$Fo = \frac{\alpha_g \tau_0}{D^2} \quad . \qquad (11)$$

Indeed, according to Eqs. (4) and (11), one has

$$\frac{\tau}{\tau_0} = \frac{\tau^*}{Fo} \quad . \qquad (12)$$

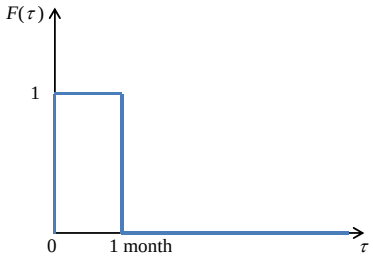

Fig. 1. Step function with a duration of one month, given by Eq.(7).

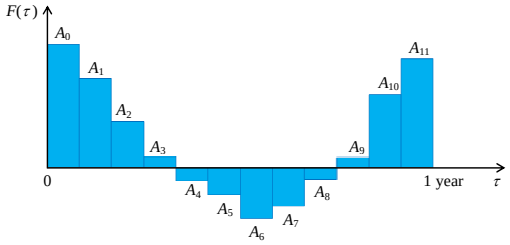

Fig. 2. Weighted superposition of twelve one-month step function, according to Eq.(9).

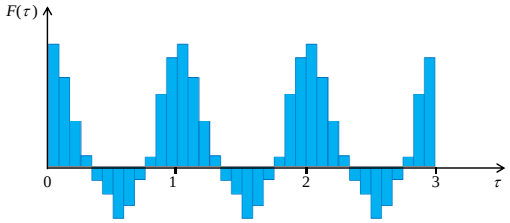

Fig. 3. Time periodic heat load with period of 1 year, according to Eq.(10).

To determine the range of Fourier numbers to be investigated, we referred to a BHE diameter in the range 9-16 cm, which accounts for most coaxial and U-tube BHEs, and to the typical values of the ground thermal diffusivity α_g, as reported in Ref. [1]. As a consequence of this analysis, we chose the values Fo = 2500, 4400, 6300.

Equations (5), (6), (7), with the initial condition T^* = 0 and the adiabatic condition at the external boundary, were solved by finite element computations performed through the software COMSOL Multiphysics. In detail, the Heaviside function *flc2hs* available in COMSOL Multiphysics was used to model Eq.(7), and a uniform dimensionless time step equal to

$(50/16000)\cdot \tau^* / Fo$ was adopted in the simulations.

Table 1. Values of $T^*_{S_B}$ for several values of τ^* / Fo, evaluated with 3 meshes.

τ^*/Fo	$T^*_{S_B}$ Mesh 1	$T^*_{S_B}$ Mesh 2	$T^*_{S_B}$ Mesh 3
0.1	1.430E-01	1.409E-01	1.405E-01
0.5	1.467E-02	1.438E-02	1.429E-02
1	7.302E-03	6.772E-03	6.734E-03
2	3.701E-03	3.570E-03	3.236E-03
5	1.562E-03	1.557E-03	1.422E-03
10	7.944E-04	8.000E-04	7.719E-04
20	3.858E-04	3.870E-04	3.899E-04
50	1.474E-04	1.480E-04	1.500E-04

Table 2. Values of T^* at a distance of 160 diameters from the BHE axis for several values of τ^* / Fo, evaluated with 3 meshes.

τ^*/Fo	T^* Mesh 1	T^* Mesh 2	T^* Mesh 3
0.1	9.925E-09	4.696E-09	6.719E-09
0.5	6.139E-04	5.966E-04	5.962E-04
1	1.447E-03	1.531E-03	1.528E-03
2	1.576E-03	1.601E-03	1.637E-03
5	1.061E-03	1.063E-03	1.032E-03
10	6.476E-04	6.513E-04	6.372E-04
20	3.497E-04	3.507E-04	3.527E-04
50	1.433E-04	1.439E-04	1.457E-04

The mesh independence of the results was checked by comparing the time evolution of the dimensionless temperature, evaluated on S_B and at a distance of 160 diameters from the BHE axis, obtained by employing 3 unstructured triangular meshes: Mesh 1, with 8176 elements; Mesh 2, with 12064 elements; Mesh 3, with 26624 elements. The results of the comparison are reported in Tables 1 and 2 for some values of τ^* / Fo: the discrepancies between the results are always very small.

With reference to the dimensionless temperature on S_B, the mean square deviation with respect to Mesh 3 is 0.000925 for Mesh 1 and 0.000201 for Mesh 2, and the relative mean square deviation with respect to the mean value is 0.0442 for Mesh 1 and 0.00961 for Mesh 2. With reference to the dimensionless temperature at a distance of 160 diameters from the BHE axis, the mean square deviation with respect to Mesh 3 is 0.000038 for Mesh 1 and 0.000018 for Mesh 2, and the relative mean square deviation with respect to the mean value is 0.0513 for Mesh 1 and 0.0240 for Mesh 2.

Since the computational time is not long, Mesh 3 was adopted for final computations.

3. Results

For each value of the Fourier number *Fo*, the results of the computations are values of the dimensionless temperature T^* versus the dimensionless parameter τ^* / Fo, in the range $0 \le \tau^* / Fo \le 50$, at 11 dimensionless distances from the BHE axis, namely: $L^* = L / D = 0.5$ (*i.e.*, at the BHE surface S_B), 40, 50, 60, 70, 80, 90, 100, 120, 140, 160. By applying the space superposition of effects, the distances listed above allow to evaluate the time evolution of the mean dimensionless temperature at the surface of the most critical BHE for any BHE field (such as a single line, a double line, a square or rectangular field) that can be considered as a part of a square field having dimensionless side up to 320 (*i.e.*, about 51 m for typical U-tube BHEs and 29 m for typical coaxial BHEs) and a minimum dimensionless distance between adjacent BHEs equal to 40.

For instance, let us consider a single line of 5 BHEs with a distance between the axes of two neighbouring BHEs equal to 40 diameters. Then, the dimensionless distances involved in the evaluation of the surface temperature of the most critical BHE (the central one), are 40 and 80 and the dimensionless temperature at the BHE surface, denoted by $T^*_{1\times5}$, can be expressed as

$$T^*_{1\times5} = T^*_{S_B} + 2\,T^*_{40} + 2\,T^*_{80} \quad . \tag{13}$$

Equation (13) is evaluated with the dimensionless unit step heat load *F*; then, a proper weighted sum of the results will yield the time evolution of $T^*_{1\times5}$ corresponding to the real heat load *f* given by Eq.(10).

For each value of *Fo* (2500, 4400, 6300) and for each value of the dimensionless distance from the BHE axis (1/2, 40, 50, 60, 70, 80, 90, 100, 120, 140, 160) the dimensionless temperature T^* has been evaluated numerically

as a function of τ^*/Fo, in the range $0 \le \tau^*/Fo \le 50$, with steps of $(50/16000)\cdot\tau^*/Fo$.

Then, interpolating functions have been determined, with the structures

$$T^*_{S_B} = \begin{cases} B_1 \ \mathrm{Ln}(1+B_2\,\tau^*/Fo)\,; & 0 \le \tau^*/Fo < \dfrac{1}{12} \\ \dfrac{B_3}{(\tau^*/Fo)^{B_4}} + \dfrac{0.008}{\tau^*/Fo}\,; & \tau^*/Fo \ge \dfrac{1}{12} \end{cases}, \tag{14}$$

$$T^*_{L^*} = C_1\left[(\tau^*/Fo)^{C_2}\cdot \mathrm{Exp}\left(\frac{C_3}{\tau^*/Fo}\right)\right]^{-1};\ \tau^*/Fo > 0\,, \tag{15}$$

where $T^*_{S_B}$ is the dimensionless temperature at the BHE surface S_B and $T^*_{L^*}$ is the dimensionless temperature at the dimensionless distance L^* from the BHE axis; B_1, B_2, B_3, B_4 and C_1, C_2, C_3 are constants, whose values are reported in Tables 3 and 4, respectively.

Illustrations of the time evolution of $T^*_{L^*}$ caused by the unit step heat load F, for $Fo = 4400$, are presented in Figures 4 and 5. Figure 4 shows the dimensionless temperature $T^*_{S_B}$ at the BHE surface for the first 3 years. The plot drawn with the red line represents the computational results, while the plot drawn with the orange line represents the interpolating function. The two plots are nearly everywhere coincident, so that almost only the orange colour appears. Similarly, Figure 5 represents the time evolution of T^* at a distance of 50 diameters from the BHE axis; again, the red and orange curves are very close.

Table 3. Coefficients of the interpolating function for $T^*_{S_B}$, given by Eq. (14).

$L^* = 0.5$			
B_1	B_2	B_3	B_4
$Fo = 2500$			
0.0783	25600	1.770E-06	5
$Fo = 4400$			
0.0778	46706	5.477E-07	5.5
$Fo = 6300$			
0.0785	62935	1.645E-07	6

Table 4. Coefficients of the interpolating function for $T^*_{L^*}$, given by Eq. (15).

L^*	C_1	C_2	C_3
$Fo = 2500$			
40	0.00825	1.060	0.22
50	0.00800	1.065	0.323
60	0.00790	1.070	0.445
70	0.00777	1.071	0.586
80	0.00762	1.0711	0.738
90	0.00759	1.0712	0.92
100	0.00755	1.017	1.12
120	0.00751	1.017	1.60
140	0.00747	1.019	2.14
160	0.00746	1.019	2.75
$Fo = 4400$			
40	0.00940	1.065	0.15
50	0.00829	1.065	0.20
60	0.00798	1.066	0.27
70	0.00780	1.069	0.35
80	0.00735	1.055	0.42
90	0.00705	1.020	0.495
100	0.00700	1.010	0.60
120	0.00700	1.010	0.86
140	0.00700	1.003	1.155
160	0.00700	1.003	1.50
$Fo = 6300$			
40	0.0106	1.052	0.12
50	0.0095	1.053	0.16
60	0.0090	1.030	0.205
70	0.0084	1.015	0.25
80	0.0078	1.010	0.30
90	0.0072	1.004	0.347
100	0.0069	0.98	0.405
120	0.0066	0.94	0.549
140	0.0064	0.93	0.739
160	0.0062	0.92	0.952

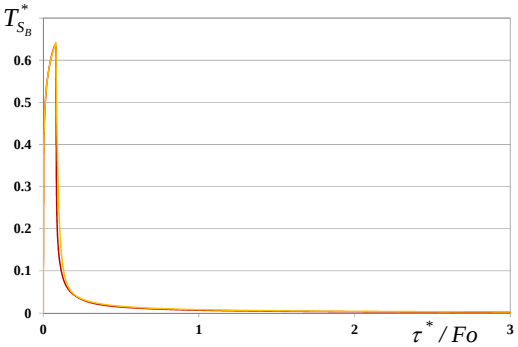

Fig. 4. Dimensionless temperature at the BHE surface, produced by F: computational values in red, interpolating function in orange.

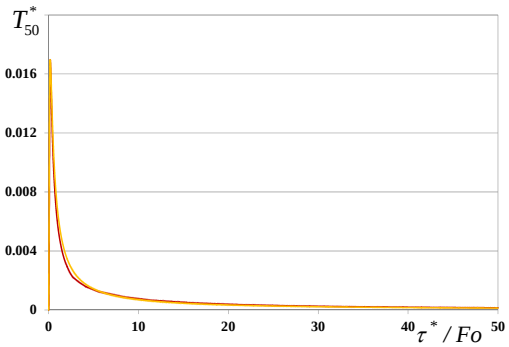

Fig. 5. Dimensionless temperature at a distance of 50 diameters, produced by *F*: computational values in red, interpolating function in orange.

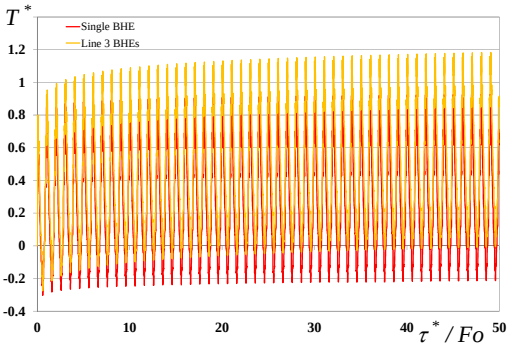

Fig. 6. Dimensionless temperature on the BHE surface, for a single BHE and for the most critical BHE in a line of 3 with a dimensionless distance equal to 40 (*Fo* = 4400).

For BHE fields in which the distance between adjacent BHEs is higher than 40 diameters (dimensionless distances less than 40 diameters are not recommendable), a linear interpolation between the coefficients listed in Tables 3 and 4 can be used, with errors less than 10% in all the conditions that we checked.

The effects of the hourly peak loads can then be added by employing the results obtained in Ref. [8], which are independent of the groundwater velocity and the BHE field geometry.

4. Examples

In this Section, some applications of the results will be illustrated. We will refer to a partially balanced seasonal heat load, with a predominant winter load. This is a common circumstance for residential buildings placed in North or North-Centre Italy. The considered dimensionless heat load is obtained by adopting the following values for the coefficients in Eq.(9):

$$\begin{aligned} &A_0 = 1, A_1 = 0.725, A_2 = 0.374, A_3 = 0.0872, \\ &A_4 = -0.11, A_5 = -0.225, A_6 = -0.417, \\ &A_7 = -0.319, A_8 = -0.101, \\ &A_9 = 0.0798, A_{10} = 0.589, A_{11} = 0.886. \end{aligned} \tag{16}$$

A plot of this heat load is represented in Figures 2 and 3.

With reference to a distance of 40 diameters between adjacent BHEs and to the intermediate value of the Fourier number, *Fo* = 4400, we will first study a line of 3 BHEs. We will compare the time evolution of the mean dimensionless surface temperature of the most critical BHE in the field (*i.e.*, the central one) with that of a single BHE, both obtained by means of the method explained in Section 3. The comparison is presented in Figure 6, where the red line refers to a single BHE and the orange line refers to the line of 3 BHEs. The Figure shows that a line of 3 BHEs has an acceptable long-term behaviour, even in the absence of groundwater flow. Indeed, the highest value of the dimensionless temperature (after 49.083 years) is 0.926 for the single BHE and 1.183 for the line of 3 BHEs, with a 28% relative increase.

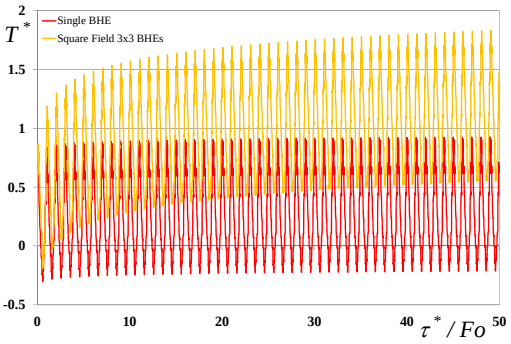

Fig. 7. Dimensionless temperature on the BHE surface, for a single BHE and for the most critical BHE in a square field of 3×3 BHEs, with a dimensionless distance equal to 40 (*Fo* = 4400).

The time evolution of surface temperature of a single BHE and of the most critical BHE for a square field of 3×3 BHEs is illustrated in Figure 7. The figure shows that the case of a square field of 3×3 BHEs is critical: the highest dimensionless temperature (after 49.083 years) is 1.831, *i.e.*, 1.98 times the value (0.926) which occurs for a single BHE. Moreover, the annual increase of the surface temperature of the most critical BHE (the central one) after 50 years is still very steep.

5. Conclusions

The time evolution of the surface temperature of the most critical BHE, for BHE fields with unbalanced seasonal loads and no groundwater movement, has been studied by finite-element computations and the superposition of effects. Two dimensionless tables have been provided, which allow a straightforward evaluation of the time evolution of the dimensionless temperature at the surface of the most critical BHE for a period of 50 years, for any BHE field, with a minimum distance of 40 diameters between adjacent BHEs, which can be considered as a part of a square field with a maximum side length of 320 diameters. For distances between adjoining BHEs higher than 40 diameters, a linear interpolation between the coefficients reported in the tables can be employed with a good accuracy.

6. References

1. S.P. Kavanaugh and K. Rafferty, Ground-source heat pumps: design of geothermal systems for commercial and institutional buildings. *ASHRAE*, Atlanta, GA, 1997.
2. *ASHRAE Handbook - HVAC Applications*, chap. 32, 2007.
3. L. Rybach and W.J. Eugster, Sustainability aspects of geothermal heat pumps. In: *27th Workshop on Geothermal Reservoir Engineering*, Stanford University, California, 2002, SGP-TR-171, p. 1-6.
4. L. Rybach, W.J. Eugster, Sustainability aspects of geothermal heat pump operation, with experience from Switzerland, *Geothermics*, **39**, 365-369 (2010).
5. S. Signorelli, T. Kohl, L. Rybach, Sustainability of production from borehole heat exchanger fields. In: *29th Workshop on Geothermal Reservoir Engineering*, Stanford, California, 2004, SGP-TR-175, p. 1-6.
6. S. Lazzari, A. Priarone, E. Zanchini, Long-term performance of BHE (borehole heat exchanger) fields with negligible groundwater movement, *Energy*, **35**, 4966-4974 (2010).
7. A.D. Chiasson, R.S. Rees, J.D. Spitler, A preliminary assessment of the effects of groundwater flow on closed-loop ground-source heat pump systems, *ASHRAE Transactions*, **106**, 380-393 (2000).
8. E. Zanchini, S. Lazzari, A. Priarone, Long-term performance of large borehole heat exchanger fields with unbalanced seasonal loads and groundwater flow, *Energy*, **38**, 66-77 (2012).